# Multiple scattering in cirrus and mixed phase mid-level ice/water clouds during CLARE'98 and implications for space lidar

**H. Flentje, Ch. Kiemle and W. Renger**
**Arbeitsgruppe Lidar, DLR-Oberpfaffenhofen, D-82234 Wessling, Germany**
**Phone : +49 8153 282525 Fax : +49 8153 281271**
**Email:** harald.flentje@dlr.de

## INTRODUCTION

The resolution and parametrisation of (sub-visible) cirrus as well as mid-level clouds in global climate models is one of the major error sources in the attempt to predict future atmospheric changes. Especially the radiative transfer in these clouds related to multiple scattering of solar and terrestrial photons is yet poorly quantified. In fact the budget of net in- and outgoing radiation from a cloud layer is quite sensitive to its optical properties which have to be derived from or parameterised according to optical measurements.
The effects of multiple scattering on remote sensing e.g. by lidar are first an increased penetration depth of the pulses into the clouds which leads to a reduction of the observed extinction. Second the path length of multiply scattered photons is longer than the single scattered path which distorts the range determination and causes a washout of the cloud's far boundary [1, 2, 3]. Platt [1] showed that for a given wavelength multiple scattering increases with cloud optical depth, cloud range, range into the cloud, cloud particle size and with the receiver field of view. This implies that there is a large amount of information convoluted in the back-scattered lidar signal. The separation of and accounting for the single contributions determining the profiles thus requires some ad hoc or experience-based assumptions i.e. a simplified model to reduce the problem's degrees of freedom.
The CLARE'98 campaign from 5 to 23 October 1998 near Chilbolton, southern UK combined ground-based and airborne lidar and radar systems as well as a comprehensive set of airborne in-situ measurements to characterise the optical and micro-physical parameters of mid-level mixed-phase clouds.

## DOUBLE SCATTERING INVERSION ALGORITHM

Though multiple scattering is less important in lidar applications than in natural atmospheric radiative transfer due to the small laser beam divergence and the narrow field of view, it nevertheless needs to be considered especially for high optical depths. An exact however very costly treatment of multiple scattering can be achieved by (stochastic) Monte Carlo techniques if they have been made feasible by variance reduction. But even so, these are not suitable for routine applications, instead numerically fast and sufficiently precise approximated models are required.

In the algorithm applied here, developed by Ruppersberg et al. [4], the multiple scattering is approximated by the double scattering term which holds if the phase function is largely dominated by forward scattering (e.g. realised in cirrus clouds consisting of large ice particles). Mathematically a double scattering term $Q_{ms}^{(2)}(r)$ is introduced into the lidar equation:

$$\Delta P(r) = P_i \Delta r A \frac{1}{r^2} \beta(r) \tau^2(r) (1 + Q_{ms}^{(2)}(r)) , \qquad (1)$$

$\Delta P(r)$ and $P_i$ denote the number of photons received in the range interval $\Delta r = c\Delta t/2$ and at a reference distance r, A being the effective receiver area, $\beta(r)$ the backscatter coefficient and $\tau(r)$ the optical depth of the atmosphere between the lidar system and the sampling interval at the distance r. The double scattering correction

$$Q_{ms}^{(2)}(r) = \frac{\Delta P^{(2)}(r)}{\Delta P^{(1)}(r)} \qquad (2)$$

is the ratio of singly to doubly scattered photons in a sampling interval. The analytical formulas for this inversion are derived by Ruppersberg et al. [1997].
The phase function of Cirrus ice crystals decreases by several orders of magnitude when going from 0 to some 10 mrad scattering angle and may be approximated by a simple exponential function. If, as the Babinet theorem (e.g. [5]) states, the diffraction lobe produces 50% of the extinction coefficient $\sigma_e$ and its width is proportional to the wavelength $\lambda$, this allows for an analytical integration of an approximate $Q_{ms}^{(2)}(r)$:

$$Q_{ms}^{(2a)}(r) \approx \Delta r \sigma_e(r_i) + \qquad (3)$$

$$\Delta r \sum_{j=1}^{i-1} \sigma_e(r_j) \left[ 1 - \left( 1 + \frac{i - 1/2}{i - j} \frac{\alpha}{\vartheta_w(\lambda, r_j)} \right) \exp\left( - \frac{i - 1/2}{i - j} \frac{\alpha}{\vartheta_w(\lambda, r_j)} \right) \right]$$

for i = 2,...,n and $Q_{ms}^{(2a)}(r_i) = 0$ at start, $\alpha$ being the receiver field of view (FOV). The 1/e-width of the phase function $\vartheta_w$,

is parameterised using Babinet's theorem by its forward scattering value at an angle of zero degrees $\beta'_{\lambda_0}$:

$$\vartheta_w(\lambda, r_p) \approx \frac{1}{2\sqrt{\pi \beta'_{\lambda_0}(0, r_p)}} \frac{\lambda}{\lambda_0}. \quad (4)$$

As an alternative quantification of the multiple scattering contribution profiles of Platt's Eta parameter [1] are shown in the Figures which supply the seemly reduction of the optical depth caused by multiple scattering.

In this article we always refer to the backscatter ratio $\gamma$ as the measure of the particle scattering:

$$\gamma = \frac{\beta_p}{\beta_m} + 1$$

$\beta_p$ and $\beta_m$ being the particle and the molecular backscatter coefficient. $\beta_m$ is calculated via the Rayleigh formula from standard profiles of temperature and pressure. Thus this quantity can easily be transformed to the particle backscatter coefficient $\beta_p(h) = (\gamma - 1)(\alpha_m(h)/8.38)$ with the Rayleigh extinction standard profile $\alpha_m(h, T, p, \lambda) = 8\pi/3 * \beta_m(h,T,p,\lambda)$ ($8\pi/3$ = lidar ratio for Rayleigh scattering). In Figure 1 the Rayleigh backscatter standard profile $\beta(h, T, p, \lambda)$ applied for the calculations presented in this article is plotted for the three wavelengths as a function of height valid for a mid-latitude standard temperature and pressure profile [9].

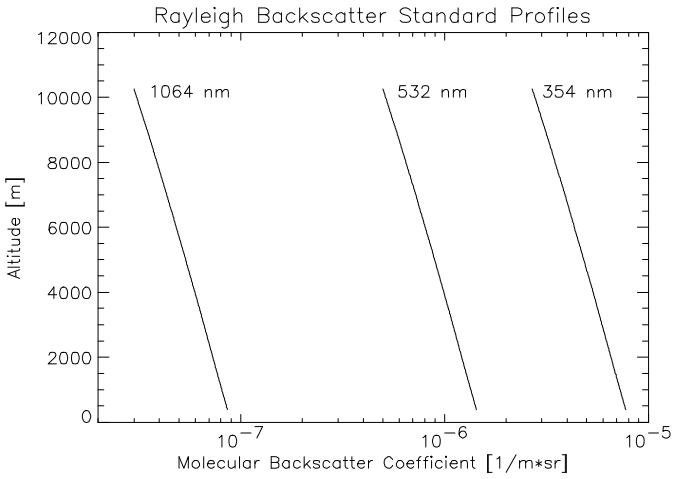


**Figure 1:** *Standard profile of the Rayleigh (molecular) backscatter coefficient calculated from the analytical formula with standard temperature and pressure profiles*

## THE BACKSCATTER LIDAR

During the CLARE'98 campaign the 3 wavelength lidar of the DLR (ALEX - see Fig. 2) was operated in down-looking mode onboard a FALCON 20 aircraft. It makes use of a Nd:YAG laser emitting at 1064nm. Frequency doubling and tripling provides 532nm and 355nm channels. The received 532nm signal is split into two perpendicularly polarised portions which allows to calculate the depolarisation of the light. With a repetition rate of 10Hz for typical aircraft speed of 150m/s the raw data resolution is about 15m horizontally.

**Table 1***: Aerosol Lidar EXperiment system parameters*

| | |
|---|---|
| Transmitter | Continuum Nd:YAG-laser NY61 |
| Wavelengths, Energy per pulse, detector | 1064 (150mJ) APD<br>532 (120mJ) PMT<br>355 (150mJ) PMT |
| Pulse lengths | 6 ns |
| Beam divergence | 0.7 mrad |
| Pulse repetition rate | 10 Hz |
| Telescope | 35 cm, Cassegrain |
| Field of view (full angle) | 1 mrad |
| Focal length | 5 m |

Vertically the ADC sampling rate results in a resolution of 15m. However, to improve the S/N ratio the compromise between signal noise and resolution leads to a respectively processed data resolution of 1–3 km horizontally and 30m vertically. The receiver is a Cassegrain telescope (r = 17.5cm) with 1mrad field of view. Performance of the lidar system and data limitations are described by [6](this issue) and on principle also by [11].

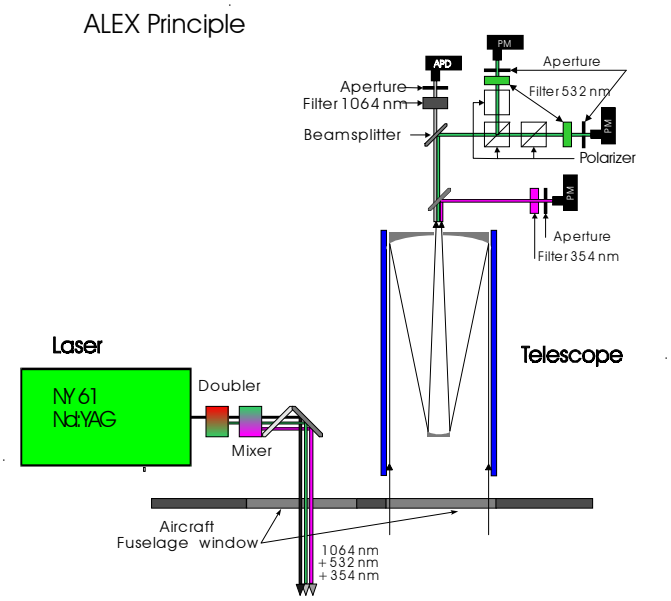


**Figure 2:** *Biaxial optical system and beam path of the ALEX lidar. Left side: transmitter, right: receiver. System parameters according to Table 1. The overlap of the laser beam and the receiver field-of-view is achieved after a distance of about 1-1.5 km.*

The attenuated atmospheric backscatter directly measured by the lidar is either given absolutely as backscatter coefficient [$m^{-1}sr^{-1}$] or relative to Rayleigh scattering (calculated from air

density) as backscatter ratio $\gamma = (\beta_{particle} + \beta_{molecule})/\beta_{molecule}$, the relative contribution of particle scattering to the total signal (cf. Figure 1). The attenuation of the laser beam in the atmosphere is considered employing a numerical inversion of (1) whereby an extinction/backscatter ratio (lidar ratio) and a starting value at some distance from the receiver has to be assumed to iteratively derive the profiles. With the inferred lidar ratio the extinction coefficient and its integral, the optical depth, can be estimated from the backscatter signal. From (3) the double scattering term $Q_{ms}^{(2)}(r)$ is calculated and fed into the inversion. The ratio of the orthogonal and parallel (to the incident beam) polarised 532nm signals $\beta_\perp / \beta_\parallel$ i.e. the depolarisation of the light by the scattering particles contains information about their sphericity. A volume depolarisation of 1.4% occurs if only the unsymmetrical air-molecules contribute to the depolarisation. If depolarising (non-spherical, solid) particles are within the measured volume the volume-depolarisation is between 0.014 and 1 depending on the concentration and shape of the scattering particles. Clouds with *only* spherical (liquid) particles may cause volume-depolarisation ratios below 1.4% since they increase only the intensity in the parallel channel.

## DATA EVALUATION

The double scattering inversion algorithm of Ruppersberg et al. [4] has been applied to clouds of different type and density observed during the CLARE'98 campaign to derive the approximate multiple scattering factor and the optical depth of the clouds simultaneously. However the extinction coefficient is not determined independently but calculated via the inferred backscatter/extinction ratio (lidar ratio). This quantity is changed incrementally during the inversion to approach a backscatter ratio beyond the clouds which is known or may be estimated (e.g. from a standard atmospheric profile). If the multiple scattering contribution is neglected or underestimated a wrong lidar ratio results from the inversion. Thus the inferred lidar ratio tends to get abnormally high if relevant scattering orders are neglected (this effect is especially strong in the classical single scattering inversion).

The total optical depth (one way) penetrated by the laser beam in practice is limited to a value of $\tau \approx$ 2-3 depending on the adjustment and the energy distribution between the three wavelength channels. However the inversion of the signal remains stable only for optical depths $\tau <$ 1-1.5. This limits our study to optically thin or shallow dense clouds.

As quoted above there are now several optical- and system-parameters known to determine whether and to what extent higher scattering orders are relevant for a given optical system. Namely the wavelength, the optical depth $\tau$, the cloud type (i.e. the particle size distribution) and the range into the cloud varied (either naturally or operationally) during the flights. The dependence of $Q_{ms}^{(2)}(r)$ on the cloud range is briefly discussed comparing airborne and satellite borne cloud observing systems [10].

We first will discuss the correlation between multiple scattering (approximated by double scattering) and the optical depth of the clouds. The cloud density typically varied along the lidar sections allowing consecutive measurements in clouds of the same type. However in most cases the density soon exceeded the penetration depth of the laser beam. For the less dense clouds the relation between optical depth and the double scattering factor is compared for different cloud types.

Though the unknown phase function of the clouds is a general source of error the authors of [4] conclude that using phase functions of a wrong cloud type for optical depths $\tau < 1$ and a FOV of 1mrad has only a minor effect on the retrieved optical depth and the multiple scattering contribution. To check the sensitivity of the results, test inversions based on phase functions for different cloud size distributions were performed. The according phase functions have been taken from [4] and in order to check their range interval also derived from model distributions of major cloud classes established by Carrier et al. [7] based on an extensive literature survey. The model distributions were approximated by log-normal-functions for which Mie calculations provided the value at a scattering angle of zero. This is sufficient since in the applied algorithm the phase function is parameterised by its forward value $\beta'_{\lambda_o}(0, r_p)$ assuming an exponential decrease around 0° and that 50% of the attenuation is due to the diffraction lobe. If not otherwise noted, we apply forward values $\beta'_{\lambda_o}$ = 20000/sr, 8550/sr and 2500/sr of the phase function at 355 nm, 532 nm and 1064 nm, respectively .

## MEASUREMENTS AND RESULTS

*Meteorological situation*: Throughout the FALCON-campaign the synoptic situation in western Europe was dominated by a pronounced westerly current in which short wave disturbances in rapid succession affected South Britain. The associated fronts passed nearly daily and caused distinct air-mass transitions between the pre- and post frontal flows. Thus overcast and alternating conditions prevailed with multi-level clouds frequently occurring throughout the troposphere. On 12 October Chilbolton was lying inside a north-westerly flow of relatively instably stratified maritime sub-polar air (mP) which, getting into the warm sector of the Iceland cyclone SASKIA, on 13 Oct was replaced by humid maritime sub-tropical (mS) air-masses. In its cold sector again mP air interspersed (15 Oct), before after temporary mS advection on 16/17 Oct maritime arctic air (mA) reached Chilbolton in a high-reaching northerly flow on 18 Oct. Following it turned westwards and transformed into mP air by 20 Oct. On 21 Oct the warm sector of the North Atlantic low VALERIE II initiated another upsliding motion of mS air-masses.

From the 5 flight missions of the CLARE'98 campaign a number of clouds were investigated in terms of their multiple scattering contribution. Two representative measurements were selected for detailed cases studies, the 5$^{th}$ leg on 14 October (about 13:06 UT) and the 2$^{nd}$ leg on 20 October (about 09:46 UT), 1998. Then moderately dense clouds of different type were observed which varied in optical depth

along the flight path but were optically thin enough to be penetrated by the lidar beam. On *14 October 98* around 1300 UT the front associated with the cold sector of the cyclone SASKIA had just passed and extended cirrus were observed between 6.8 and 8.3km height with backscatter ratios larger than 1000 at 1064 and 120 and 532nm as shown in Figure 4. In its denser regions the volume depolarisation was about 20-50%. The top of the boundary layer is marked by low diminishing stratus/stratocumulus near 1000m above the ground.

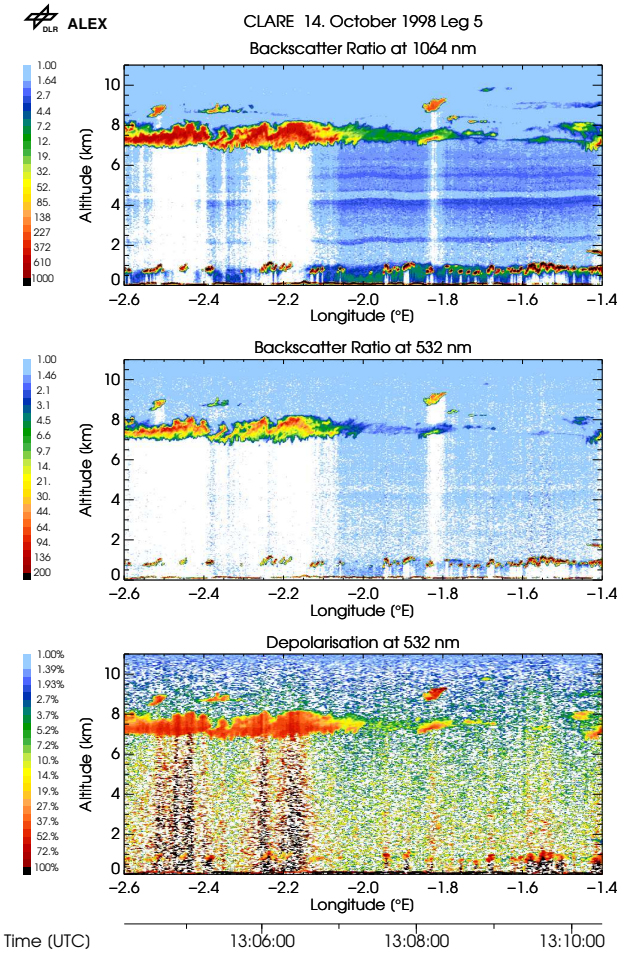


**Figure 3:** *Sections of backscatter ratio at 1064 nm (upper panel) at 532nm (middle panel) and volume depolarisation (@532nm) along the FALCON flight path on 14 October 1998, 13:04 UT – 13:10 UT. Not corrected for extinction!*

For three relatively homogenous regions of this cirrus, profiles of the (cumulative) optical depth and the double scattering factor resulting from the inversion at the three wavelengths 1064 nm, 532 nm and 355 nm are shown in Figures 3a, 3b and 3c. The profiles are each averaged over 10 - 20 s (each the same at the different wavelengths) which is about 2-4 km horizontally or 0.03-0.06° in longitude. The optical depth of the cloud between about 6.8 and 8.2 km is nearly the same at the three wavelengths ($\tau \approx 0.5$ at 13:04:29 (-2.54°E), $\tau \approx 0.7$ @13:06:18 (-2.2°E) and $\tau \approx 0.03$ @13:06:58 (-2.07°E)) as is expected for a cirrus cloud with particles much larger than the wavelengths. Even at 13:06:58 UT where most of the attenuation at the short wavelengths occurs outside the cloud the optical depth is nearly wavelength independent.

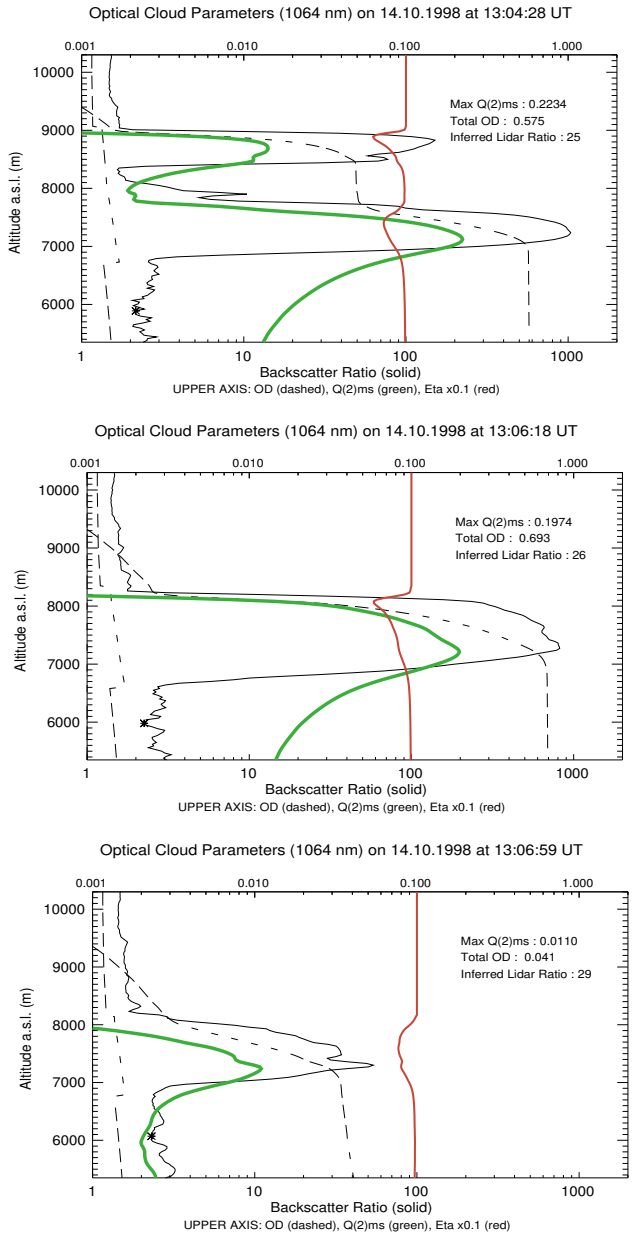


**Figure 4a:** *Vertical profiles of backscatter ratio BSR (solid), optical depth (dashed), double scattering factor $Q_{ms}^{(2)}(r)$ (green) and Platt's Eta (red) at 1064 nm on 14 October 13:04:28, 13:06:18 and 13:06:59 (cf. Fig. 2). The corresponding longitudes are –2.54°E, -2.2°E and –2.07°E, respectively. The optical parameters (upper right corner) are inferred using a cirrus phase function. $Q_{ms}^{(2)}(r)$ is plotted only below the top of the investigated cloud. The most left (dashed) line shows the BSR of the standard profile whereby the interval, in which a special lidar ratio for the cloud is assumed, is enhanced by the ratio of in-cloud/out-of-cloud lidar ratio. The asterisk indicates the altitude where the reference value is prescribed.*

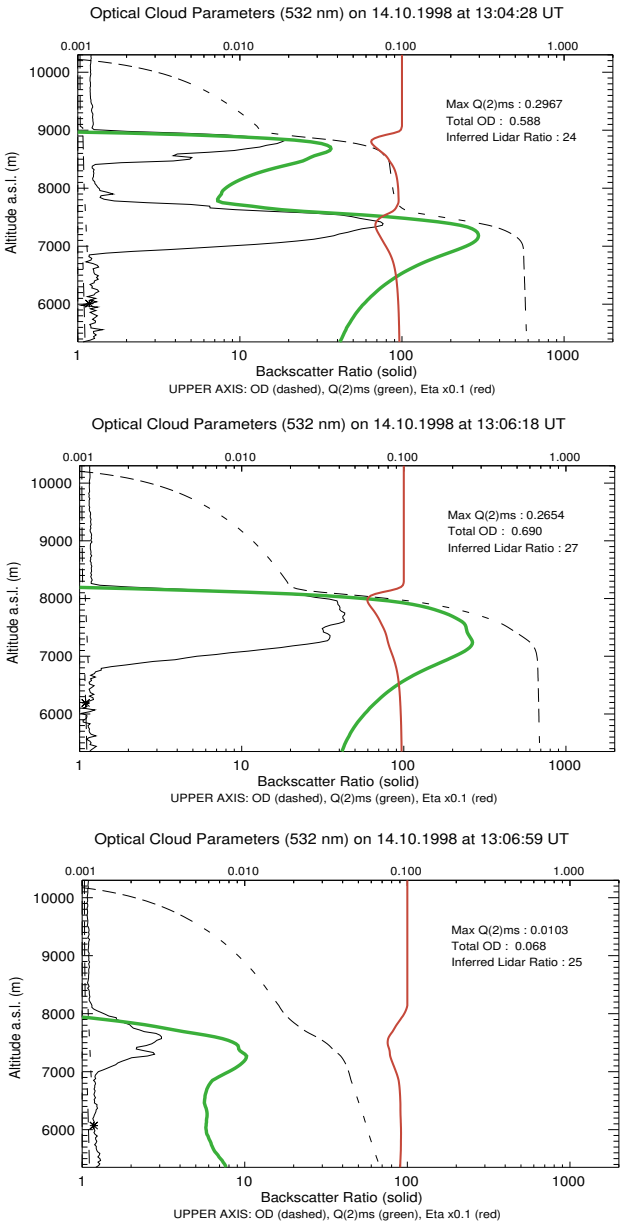


**Figure 4b:** *Vertical profiles of backscatter ratio (solid), optical depth (dashed), double scattering factor $Q_{ms}^{(2)}(r)$ (green) and Platt's eta (red) at 532 nm on 14 October 13:04:28, 13:06:18 and 13:06:59 ( Fig. 3) as in Figure 4a.*

On the contrary the optical depth below the cloud is clearly negatively correlated to λ (from 5 – 6.8 km: $\tau \approx 0.006$ @1064 nm, $\tau \approx 0.025$ @532 nm, $\tau \approx 0.06$ @355 nm) due to much smaller (aerosol) particles which are apparent as stratified layers in the upper panels of Figure 3.

However the vagueness of the lidar ratio (i.e. the inferred backscatter / extinction ratio used to calculate τ from β) is a considerable source of uncertainty. If the extinction correction which feeds into the calculation of the backscatter profile is small in the case of optically very thin clouds than the inversion of such profiles supplies only a vague determination of the free parameters, which in our case is the lidar ratio. Otherwise, if too strong scattering occurs inside one layer the signal becomes saturated or multiple scattering of higher orders occurs both of which can be compensated by assuming an erroneous lidar ratio to supply a backscatter profile which matches the prescribed reference values in the cloud free regions. However, then the extinction coefficient or the optical depth of that layer can not be determined via the lidar ratio but at most from the jump of the signal across the cloud if the atmospheric conditions are accurately known. The rather high lidar ratios of about 25 inferred for the cirrus in the infrared and green channel may presumably be due to reflection at the horizontally oriented ice crystals.

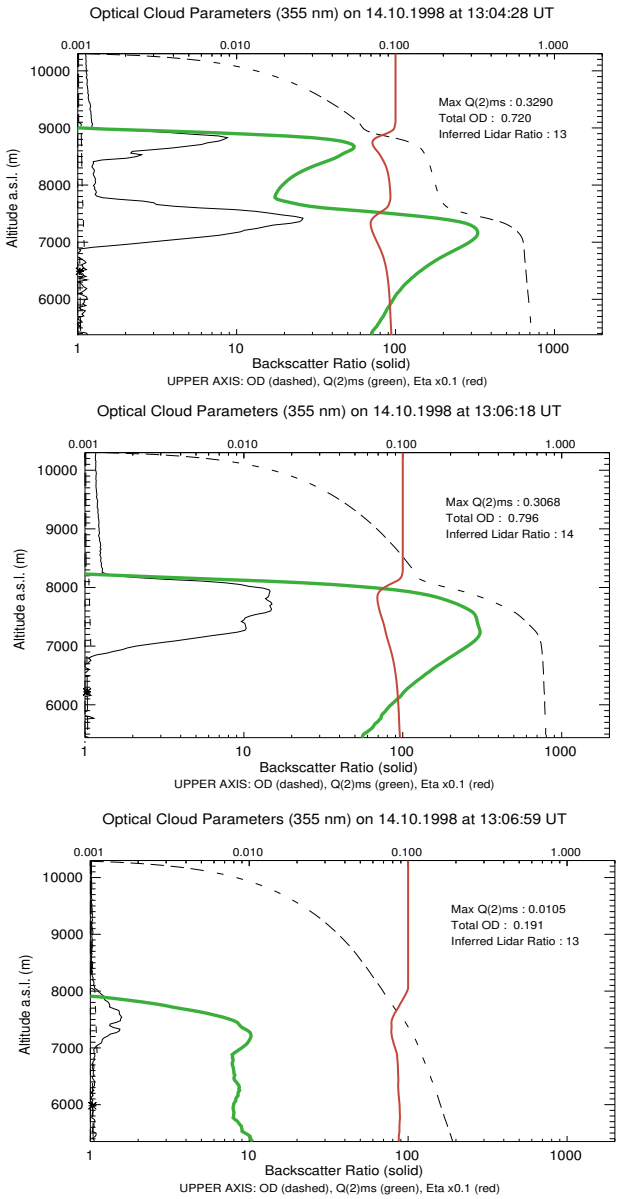


**Figure 4c:** *Vertical profiles of backscatter ratio (solid), optical depth (dashed), double scattering factor $Q_{ms}^{(2)}(r)$ (green) and Platt's Eta (red) at 355 nm on 14 October 13:04:28, 13:06:18 and 13:06:59 ( Fig. 3) as in Figure 4a.*

Our inversion allows to choose two height intervals with different lidar ratios, one of which we always set to an average background tropospheric value of 48 ([4]). The other one is chosen within the cloud of interest and acts as free parameter for the inversion. To concentrate on the selected cloud layer the double scattering factor $Q_{ms}^{(2)}$ (r) is calculated and plotted starting at the top of this cloud.

$Q_{ms}^{(2)}$ (r) increases with decreasing wavelength λ. Its mean value increases with the optical depth of the cloud (see Table 2). It reaches its highest value near the cloud base and at 1064 nm decreases by about an order of magnitude l 1000 m below the cloud. This decrease is slower at smaller wavelengths. Though we sometimes refer to the maximum value of $Q_{ms}^{(2)}$ (r) its mean value over the cloud, given in Table 2, actually is the relevant quantity for the multiple scattering contribution. The apparent reduction of the optical depth caused by the multiple scattering in this cirrus as expressed by Platt's Eta parameter ([1]) is in the order of 20-40% and varies only slightly with wavelength (see Table 2) except its gradual increase below the cloud which is slower at the short wavelengths. It tends to have a minimum just below the cloud top.

**Table 2:** *Optical cloud parameters for cirrus on 14 October 98 at 1306 UT: Optical depth τ, Mean value of Q inside the cloud and minimum value of Platt's Eta @ 1064, 532 and 355 nm*

| Time | Type- λ | τ | Mean $Q_{ms}^{(2)}$ | Min $\eta_{Platt}$ |
|---|---|---|---|---|
| 13:04:33 | Ci – 1064 | 0.53 | 0.088 | 0.72 |
| 13:06:18 | Ci – 1064 | 0.69 | 0.102 | 0.58 |
| 13:06:58 | Ci – 1064 | 0.03 | 0.005 | 0.76 |
| 13:07:30 | Ci – 1064 | 0.01 | 0.001 | 0.93 |
| 13:04:33 | Ci – 532 | 0.51 | 0.163 | 0.69 |
| 13:06:18 | Ci – 532 | 0.67 | 0.17 | 0.60 |
| 13:06:58 | Ci – 532 | 0.03 | 0.006 | 0.75 |
| 13:07:30 | Ci – 532 | 0.02 | 0.002 | 0.92 |
| 13:04:33 | Ci – 355 | 0.54 | 0.193 | 0.70 |
| 13:06:18 | Ci – 355 | 0.70 | 0.205 | 0.69 |
| 13:06:58 | Ci – 355 | 0.03 | 0.006 | 0.77 |

On *20 October 98* two FALCON missions took place in the morning and in the early afternoon. Starting before noon a rapid formation of cirrus was observed above 8 km height due to the approaching occluded cold front of low VALERIE II. In a strong westerly current (≈ 15 m/s) a narrow altostratus cloud layer in 3.8 – 4.2 km altitude appeared above a dense stratocumulus cloud cover at the top of the boundary layer near 2 km and persisted in the Chilbolton flight corridor until the afternoon (see Figure 3 in [8], this issue). At that time it was tilted vertically by nearly 2 km in height over the distance of one leg (1.5°).. This altostratus layer blocked the lidar beam nearly completely such that a data evaluation below it is not possible except for parts of the first three flight legs where the cloud cover was still broken (near -1.8°E of the selected leg 2 from 09:43 to 09:50 in Figure 5). This region where the cloud covers were broken moved eastward with little change during the consecutive legs. A thin cirrus above (7.8 – 8.7 km) only exhibits maximum optical depths of $\tau \approx 0.1$ and thus does not influence the inversion of cloud parameters below it.

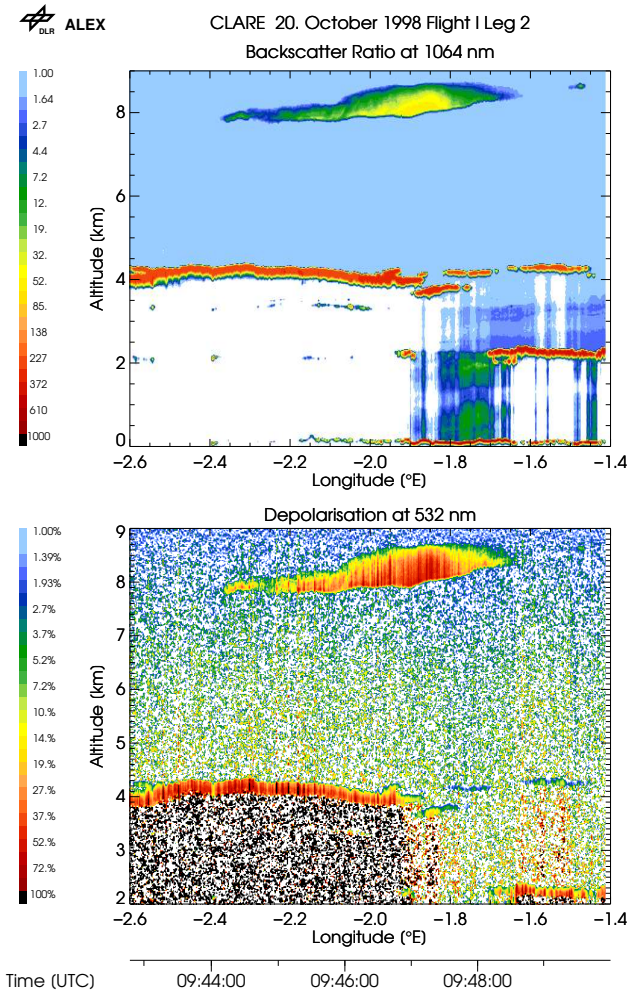


**Figure 5:** *Sections of backscatter ratio at 1064 nm (upper panel) and at 532nm (middle panel) and volume depolarisation (@532nm) along the FALCON flight path on 20 October 1998, 09:43 UT – 09:50 UT. Not corrected for extinction!*

The cloud situation at this time was already very similar to that several hours later which is one of the high priority cases defined by the CLARE community and which is referred to by several other studies in this issue. However, since at that time our lidar measurements suffered from strong attenuation in a thick cirrus cloud above 9 km altitude we concentrate on the previous flight. We expect that the micro-physical properties of this cloud moving at a constant altitude of about 4 km remained approximately unchanged between 09:48 and 14:20 suggesting that the early afternoon micro-physical measurements are also representative for the cloud stage in the morning. At 14:20 this altostratus cloud cover has been intensively investigated with different radars, lidars and airborne in situ probes installed onboard a Hercules C-130

aircraft. The layer dispersed and dissolved over Chilbolton around 14:40 UT when it has been embedded in a thick cirrus. In Figure 6 the change of the temperature profile between 10 UT and 14 UT is shown. It indicates the advection of a narrow layer of relatively warm (mP) air sliding up onto the colder (mA) air-mass (occlusion with warm front character). The associated drying of the 2 – 4 km level lead to the observed vanishing of the altostratus layer around 1440 UT. Simultaneously the overlying air-mass was lifted over the condensation level by the upsliding motion as indicated by rapid cirrus formation.

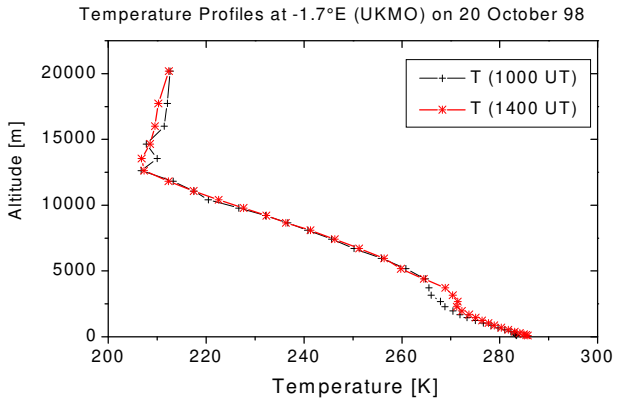


**Figure 6:** *Temperature Profiles on 20 October 1998 from UKMO at 1000 UT and 1400 UT. Labile stratification dominates over most of the troposphere. Warm advection leads to development of an inversion in about 2 km altitude.*

The low volume depolarisation ratio of the altostratus cloud of about 5% apparent in Figure 4 indicates that it contained a large fraction of spherical i.e. liquid particles (the high depolarisation west of –1.9°E is an artefact due to saturation of the parallel 532 nm signal and likely also to depolarising multiple scattering). The mixed-phase nature of this cloud is confirmed by in situ micro-physical measurements of the particle probes onboard the Hercules C-130. Accordingly at a temperature of –8.6°C in 4 km a mixture of ice crystals, graupel and water droplets was observed. A more detailed description of these measurements is given in [8].

The altostratus exhibits (extinction corrected) backscatter ratios of more than 1000 (in regions where the signal was saturated – not shown) in the infrared, up to 300 in the green and up to 70 in the blue wavelength region (Figures 7a-c). In the dense regions of the cloud the signal is saturated - especially in the IR (i.e. the capacity of the data acquisition is exceeded). Thus the double scattering contribution cannot be quantified there. The signal in the low wavelength channels was severely attenuated and are thus very noisy below the cloud. As with the cirrus discussed before, the optical depth does only slightly depend on the wavelength. In its denser regions (west of –1.9°E) the cloud cover reaches optical depths of $\tau > 1.5$ while e.g. the section near –1.7°E in 4.2 km exhibits $\tau \approx 0.1$ only.

Since this cloud contains a major fraction of liquid particles next to solid and crystal like ones, the inversion has been carried out with either an ice cloud - and a water cloud phase function, representing a cirrus and a Deirmendjian-C1 water cloud distribution with forward scattering values $\beta'_{\lambda_o}$ ($\beta'_{\lambda_o}$ = 2650/sr @355 nm, $\beta'_{\lambda_o}$ = 210.2/sr @550 nm, $\beta'_{\lambda_o}$ = 60.5/sr @1064 nm) taken from [4] (extrapolated quadratically for 355 nm).

The cloud optical depth as well as the double scattering factor averaged over the cloud and the calculated reduction of $\tau$ as expressed by Platt's Eta parameter, are given in Table 3a for the Deirmendjian-C1 phase function and in Table 3b using the ice crystal phase function. Again, as for the cirrus discussed before, $Q_{ms}^{(2)}(r)$ increases in the cloud down to the cloud base. However it decreases more rapidly below the cloud. This drop below the cloud is even larger if we use the water cloud phase function $\varphi_w$ (Figure 7a-c) rather than the ice phase function $\varphi_{Ci}$. Applying $\varphi_{Ci}$ to the double cloud layer near –1.8°E, the double scattering contribution increases stepwise at the single layers due to the slow degradation of $Q_{ms}^{(2)}$ below each cloud while this effect misses if $\varphi_w$ is used (second panel in Figures 6b and c). It reaches quite high values $Q_{ms}^{(2)} > 0.6$ with $\varphi_{Ci}$ ($Q_{ms}^{(2)} > 0.3$ with $\varphi_w$) and likely becomes even larger in the regions which are not accessible to our study.

The retrieved optical depth depends only weakly on the selected phase function. But the calculated double scattering factors varied for more than 100% when applying the described phase functions. For a comparable optical depth there is considerably more double scattering in the mixed-phase cloud than in the cirrus if $\varphi_{Ci}$ for ice crystals is used while from applying $\varphi_w$ representing water clouds slightly smaller values result (see Tables 2 and 3a,b). This is plausible because for the broader function $\varphi_w$ a larger part of the diffraction cone is out of the receiver FOV and thus does not contribute to the received doubly scattered signal.

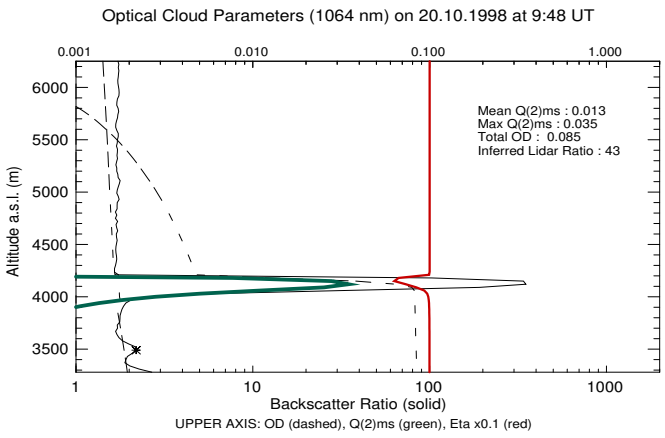


**Figure 7a:** *Vertical profiles of backscatter ratio (solid), optical depth (dashed), double scattering factor $Q_{ms}^{(2)}(r)$ (green) and Platt's Eta (red) at 1064 nm on 20 October 09:48 UT at –1.73°E ( Figure 4) as in Figure 4 but with water cloud phase function.*

Since we are dealing with a mixed phase cloud it may be expected that a combination of both phase functions is the best approximation to the actual one. With this assumption the actual dependence of $Q_{ms}^{(2)}(r)$ on the optical depth does not differ significantly for the cirrus and the altocumulus cloud. However, it turns out to be quite important to choose an appropriate phase function whereby the ones selected here already cover a broad spectrum of ambient cloud types.

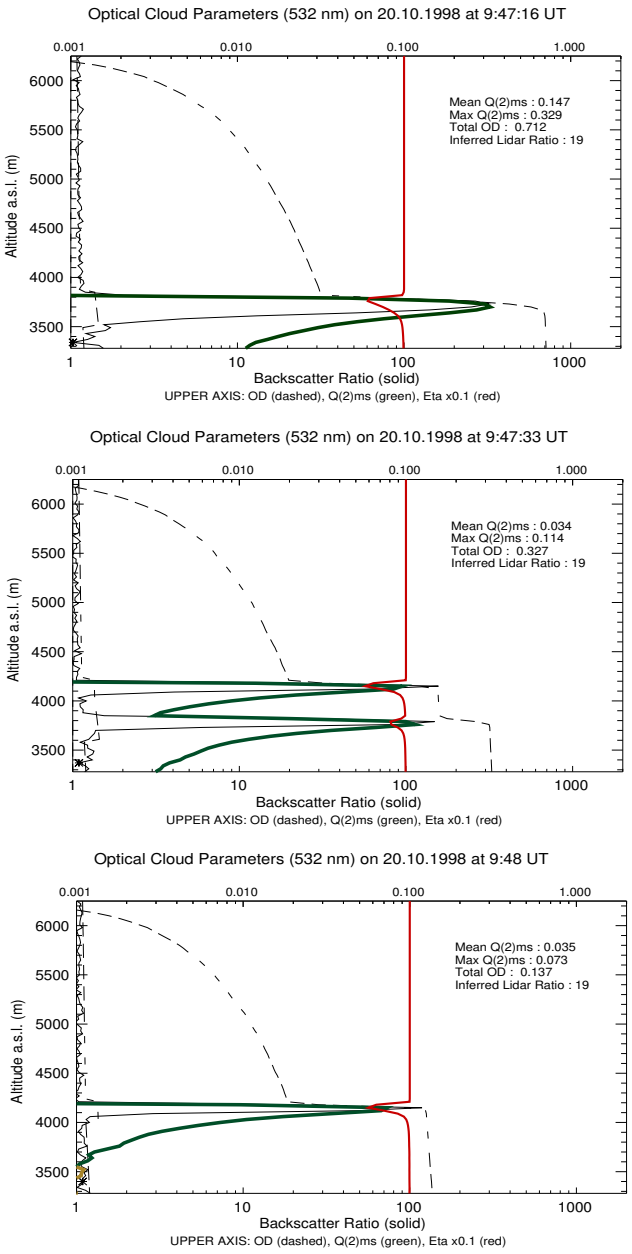


**Figure 7b:** *Vertical profiles of backscatter ratio (solid), optical depth (dashed), double scattering factor $Q_{ms}^{(2)}(r)$ (green) and Platt's Eta (red) at 532 nm on 20 October 09:47:17, 09:47:33 and 09:48:00 UT as in Figure 4 but using a water cloud phase function. The corresponding longitudes are –1.85°E, -1.8°E and –1.73°E, respectively.*

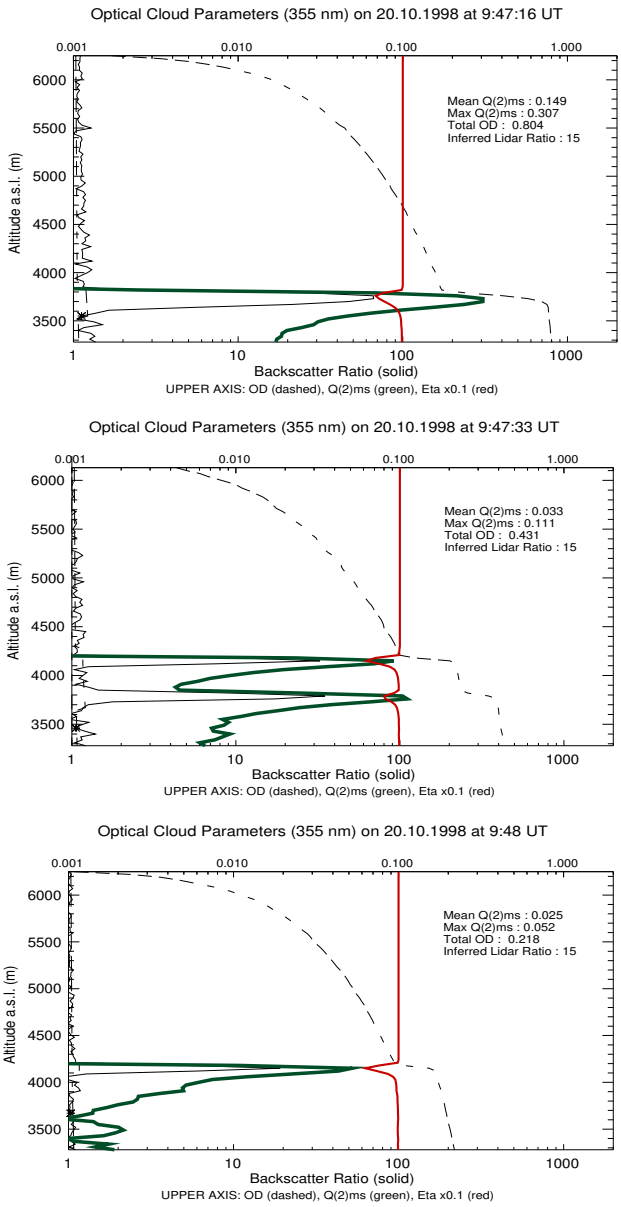


**Figure 7c:** *Vertical profiles of backscatter ratio (solid), optical depth (dashed), double scattering factor $Q_{ms}^{(2)}(r)$ (green) and Platt's Eta (red) at 355 nm as in Figure 6b.*

**Table 3a:** *Optical parameters for altocumulus cloud cover on 20 October 98 at 0946 UT: Optical depth τ, Mean value of Q inside the cloud and minimum value of Platt's Eta @ 1064, 532 and 355 nm. A Deirmendjian-C1 water cloud phase function was used.*

| Time | Type- λ | τ | Mean $Q_{ms}^{(2)}$ | Min $\eta_{Platt}$ |
|---|---|---|---|---|
| 09:48:00 | Ac – 1064 | 0.09 | 0.013 | 0.61 |
| 09:47:16 | Ac – 532 | 0.71 | 0.15 | 0.6 |
| 09:48:00 | Ac – 532 | 0.14 | 0.06 | 0.53 |
| 09:47:16 | Ac – 355 | 0.80 | 0.15 | 0.69 |
| 09:48:00 | Ac – 355 | 0.22 | 0.025 | 0.51 |

**Table 3b**: *Optical parameters for altocumulus cloud cover on 20 October 98 at 0946 UT like in Table 3a but calculated using a cirrus cloud phase function.*

| Time | Type- $\lambda$ | $\tau$ | Mean $Q_{ms}^{(2)}$ | Min $\eta_{Platt}$ |
|---|---|---|---|---|
| 09:48:00 | Ac – 1064 | 0.08 | 0.034 | 0.66 |
| 09:47:17 | Ac – 532 | 0.72 | 0.38 | 0.6 |
| 09:48:00 | Ac – 532 | 0.09 | 0.06 | 0.56 |
| 09:47:17 | Ac – 355 | 0.7 | 0.39 | 0.63 |
| 09:48:00 | Ac – 355 | 0.09 | 0.06 | 0.62 |

*EXTRAPOLATION TO A SATELLITE BORNE LIDAR SYSTEM*:
On 14 October the flight level of the FALCON was 11570 m a.s.l. thus the cloud - receiver distance ranged from 3270 to 4770 m for the near and far cloud boundary. The flight level on 20 Oct 9:46 UT was about 10280 m a.s.l. resulting in a cloud - receiver distance of 6 – 6.3 km. With 1 mrad FOV this corresponds to a (approximately) cylindrical cloud region with a diameter of about 3-6 m contributing to the received signals. At space distances (d ≈ 700 km) the cloud area visible by a 1 mrad FOV receiver has a diameter of approximately 700 m. Thus the FOV volume detected by the telescope is approximately proportional to the square of the cloud – receiver distance. However, the scattering phase function of particles much larger than the wavelength largely peaks in the forward direction. Thus the larger the particles the less the multiple scattering contribution depends on this target area. In the following we will derive a rough estimate of how much more a satellite borne instrument would suffer from multiple scattering than an aircraft borne system.
We assume a homogeneous cloud layer of 1 km depth containing no absorbing particles ($\sigma_e = \sigma_s$) in which for the given geometry the double scattering approximation of [4] is valid. Let this cloud be hit by a non-divergent laser beam from an airborne (d = 6km) and a satellite borne (d = 700 km) lidar with a FOV of few mrad each. It may consist of either ice crystals or water droplets with a diffraction lobe 1/e-width of $\vartheta_i$ = 6 mrad and $\vartheta_w$ = 36 mrad (@ 1064 nm), respectively. To get an upper limit estimation of the distance effect let all scattering occur at the cloud top (near side) as illustrated (strongly jolted) below, where the FOV volumes of the two lidar systems are outlined as cylinders of different radii.

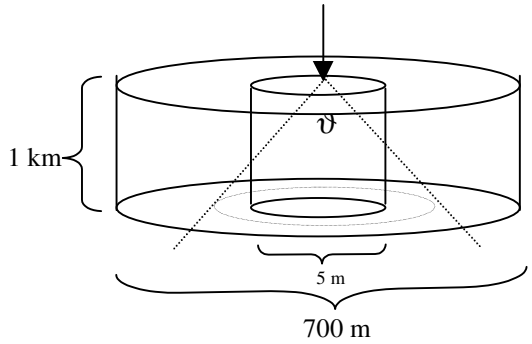


It is obvious that the deeper (in mean) inside the cloud the scattering events occur the smaller the difference in the multiple scattering contributions to the received signals will be. Geometrical considerations show that as long as the $\vartheta$-cone (defined by the 50% decrease of $\varphi$) lies within the airborne lidar FOV (inner cylinder) there would be hardly more scattered photons detected by the satellite system because the forward-scattered photons once diverted from the incident beam are mostly lost after the following back-scattering. The same is true for the broader phase function as well as long as one confines to twice scattered photons.
If on the other hand the scattering medium is diffusive (i.e. its geometrical thickness is much larger than the mean free path of photons) it may as a first approximation be regarded as isotrope source of multiply scattered photons and $Q_{ms}(r)$ then becomes dominated by the viewed cloud area rather than by other parameters. The intermediate domain of moderate multiple scattering is not accessible to simple analytic considerations. Instead the estimation of the difference in the multiple scattering impact then needs numeric efforts like Monte-Carlo- or ray-tracing techniques.

## SUMMARY

From 12 – 21 October 1998 the ALEX lidar onboard a FALCON 20 aircraft participated in the CLARE'98 campaign flown on a SW-NE orientated corridor near Chilbolton in South Britain. During the 5 flights of the campaign different types of multiply layered clouds were measured. In this article we discuss two different cloud types, a cirrus observed on 14 October and an altocumulus mixed-phase cloud from 20 October, in terms of the double scattering contributions (as approximation to multiple scattering) to the received signals. The optical depths of the investigated cloud regions ranged over about $0 \le \tau \le 0.8$. The double scattering factor $Q_{ms}^{(2)}(r)$ strongly depends on the cloud's optical depth and the wavelength. It reaches typical values of $0\% < Q_{ms}^{(2)}(r) < 60\%$ of the single scattered intensity and does not depend on the wavelength. It increases with the distance into the cloud, reaches its maximum near the cloud base and slowly decreases beyond the cloud. The decrease strongly depends on the applied phase function. If one deals with mixed phase or water clouds the selection of a scattering phase function for a wrong cloud type causes substantial errors in the double scattering contribution $Q_{ms}^{(2)}$. But though for the discussed altocumulus cloud an uncertainty of more than a factor of two in $Q_{ms}^{(2)}$ has been derived this causes only a small error in the retrieved backscatter profile since the factor $(1 + Q_{ms}^{(2)})$ feeds into the lidar equation.

## REFERENCES

[1] Platt, C.M.R., Lidar and Radiometric Observations of Cirrus Clouds, J. Atm. Sci., 30, 1191-1204, 1973.

[2] Nicolas, F., L.R. Bisonette and P. H. Flamant, Lidar effective multiple scattering coefficients in cirrus clouds, Appl. Optics, 36, 15, 3458-3468, 1997.
[3] Wandinger, U., Multiple scattering influence on extinction- and backscatter-coefficient measurements with Raman and high-spectral resolution lidars, Appl. Optics, 37, 3, 417-427, 1998.
[4] Ruppersberg, G.H., M. Kerscher, M. Noormohammadian, U.G. Oppel and W. Renger, The Influence of Multiple Scattering on Lidar Returns by Cirrus Clouds and an Effective Inversion Algorithm for the Extinction Coefficient, Contr. Atmos. Phys., 70, 2, p. 91-107, 1997.
[5] v.d.Hulst, H.C., Light scattering by small particles, John Wiley & Sons, Inc., New York, 1957.
[6] Mörl, P., M.E. Reinhardt, W. Renger and R. Schellhase, The use of the airborne LIDAR system "ALEX F1" for aerosol tracing in the lower troposphere, Beitr. Phys. Atmos., 54, 401-410, 1981.
[7] Carrier, L.W. et al., Appl. Opt., 6, 1209-1216, 1967, in: E.J. McCartney, Optics of the Atmosphere – Scattering by Molecules and Particles, John Wiley & Sons, New York, 1976.
[8] Quante, M., O. Danne, H. Flentje, W. Renger and P. Francis, Cloud boundaries and structure in mixed phase mid-level clouds as deduced from ground based 95-GHz radar and airborne lidar measurements during CLARE'98, this issue.
[9] Jursa, A. S., Handbook of Geophysics and the Space Environment, United States Air Force, 1985, p. 18-7, p. 19-1
[10] Wiegner, M, U. Oppel, H. Krasting, W. Renger, C. Kiemle and M. Wirth, Cirrus measurements from a Spaceborne Lidar: Influence of Multiple Scattering, in A. Ansmann et al., Advances in Atmospheric Remote Sensing with Lidar, selected papers of the 18th ILRC, Springer, Berlin, 1996.
[11] Flentje, H., C. Kiemle, V. Wiess, M. Wirth and W. Renger, The 3 wavelength lidar ALEX and other instrumentation onboard the FALCON during CLARE'98, this issue.